Seasonal ventilation of the stratosphere: Robust diagnostics from one-way flux distributions

Clara Orbe,[1] Mark Holzer,[1,2] Lorenzo M. Polvani,[1,3] Darryn W. Waugh,[4] Feng Li,[5,6] Luke D. Oman,[6] and Paul A. Newman[6]

Received 17 May 2013; revised 4 December 2013; accepted 6 December 2013; published 13 January 2014.

[1] We present an analysis of the seasonally varying ventilation of the stratosphere using one-way flux distributions. Robust transport diagnostics are computed using GEOSCCM subject to fixed present-day climate forcings. From the one-way flux, we determine the mass of the stratosphere that is in transit since entry through the tropical tropopause to its exit back into the troposphere, partitioned according to stratospheric residence time and exit location. The seasonalities of all diagnostics are quantified with respect to the month of year (a) when air enters the stratosphere, (b) when the mass of the stratosphere is partitioned, and (c) when air exits back into the troposphere. We find that the return flux, within 3 months since entry, depends strongly on when entry occurred: (34±10)% more of the air entering the stratosphere in July leaves poleward of 45°N compared to air that enters in January. The month of year when the air mass is partitioned is also found to be important: The stratosphere contains about six times more air of tropical origin during late summer and early fall that will leave poleward of 45° within 6 months since entering the stratosphere compared to during late winter to late spring. When the entire mass of the air that entered the stratosphere at the tropics *regardless* of its residence time is considered, we find that (51±1)% and (39±2)% will leave poleward of 10° in the Nothern Hemisphere (NH) and Southern Hemisphere (SH), respectively.

Citation: Orbe, C., M. Holzer, L. M. Polvani, D. W. Waugh, F. Li, L. D. Oman, and P. A. Newman (2014), Seasonal ventilation of the stratosphere: Robust diagnostics from one-way flux distributions, *J. Geophys. Res. Atmos.*, *119*, 293–306, doi:10.1002/2013JD020213.

1. Introduction

[2] The stratosphere-troposphere exchange (STE) of mass and tracers strongly influences the chemical and radiative properties of the upper troposphere and lower stratosphere [e.g., *Morgenstern and Carver*, 2001; *Park et al.*, 2004; *Jing et al.*, 2005; *Hegglin et al.*, 2006; *Pan et al.*, 2006]. Several studies have investigated the impact of STE on tropospheric species like ozone and nitrous oxide, with *Liang et al.* [2009] finding that as much as 78% of ozone in the Arctic upper troposphere is attributable directly to transport from the stratosphere. STE has also been shown to play a key role in setting the springtime maximum of Northern Hemisphere (NH) ozone [*Danielsen and Mohnen*, 1977; *Monks*, 2000; *Stohl et al.*, 2003] and in determining the seasonal cycles of tropospheric species including Strontium-90, Beryllium-7 [*Fry et al.*, 1960; *Dibb et al.*, 1992], chloroflourocarbons, and nitrous oxide [*Nevison et al.*, 2004; *Liang et al.*, 2008].

[3] The tropical tropopause layer (TTL) is an important source of air for the stratosphere and provides the likely boundary condition for stratospheric water vapor [*Holton et al.*, 1995]. In order to understand the key role that the TTL plays in setting the distributions of water vapor and other trace species, numerous studies have documented the "tape recorder"-like propagation of seasonally varying water vapor [e.g., *Mote et al.*, 1996; *Schoeberl et al.*, 2008b] and carbon monoxide [e.g., *Randel et al.*, 2007; *Schoeberl et al.*, 2008a; *Abalos et al.*, 2012] from the tropical tropopause into the interior of the stratosphere. Few studies, however, have assessed the seasonality of stratospheric transport from the tropopause back to the tropopause. To the best of our knowledge, no studies have documented how seasonal transport variations at the tropical tropopause affect fundamental stratospheric transport time scales such as the time between entering and exiting the stratosphere. Transport through the TTL has a seasonally recurring component that is associated with the large-scale circulation and with convection; other variations occur more episodically. For example, volcanic injections of sulfur dioxide and aerosols into the stratosphere

[1]Department of Applied Physics and Applied Mathematics, Columbia University, New York, New York, USA.
[2]Department of Applied Mathematics, School of Mathematics and Statistics, University of New South Wales, Sydney, New South Wales, Australia.
[3]Department of Earth and Environmental Sciences, Columbia University, New York, New York, USA.
[4]Department of Earth and Planetary Sciences, Johns Hopkins University, Baltimore, Maryland, USA.
[5]Goddard Earth Sciences Technology and Research, Universities Space Research Association, Columbia, Maryland, USA.
[6]Laboratory for Atmospheric Chemistry and Dynamics, NASA Goddard Space Flight Center, Greenbelt, Maryland, USA.

Corresponding author: C. Orbe, NASA Goddard Space Flight Center, Greenbelt, MD 20771, USA. (clara.orbe@nasa.gov)

2169-897X/14/10.1002/2013JD020213

occur infrequently but provide the largest natural perturbations of the stratosphere, with significant impact on global surface temperatures [*McCormick et al.*, 1995]. In light of the key role that STE plays in impacting not only stratospheric and tropospheric chemistry but also surface climate, it is important that its seasonality be quantified in a robust, reproducible manner.

[4] Numerous studies have quantified STE in terms of the exchanges of ozone and water vapor because of their key roles as greenhouse gases and chemically active species in the upper troposphere and lower stratosphere [e.g., *Olsen et al.*, 2003; *Hsu et al.*, 2005; *Tang and Prather*, 2010; *Tang et al.*, 2011]. The distribution of these species is the result of the complex interplay between transport and chemistry. Therefore, to isolate the role of transport, it is important to obtain a fundamental, quantitative understanding of STE using diagnostics that are tracer independent, that is, independent of the specific source/sink distribution of any particular chemical species. To this end, several studies have focused on diagnosing cross-tropopause transport using one-way stratosphere to troposphere (S → T) and troposphere to stratosphere (T → S) air mass fluxes [e.g., *Stohl et al.*, 2000; *Wernli and Bourqui*, 2002]. *Hall and Holzer* [2003] showed, however, that unless additional constraints are imposed on where air enters/exits the stratosphere and/or how long that air spends in the stratosphere (the stratospheric residence time), these one-way fluxes are fundamentally ill defined because of an eddy-diffusive singularity at zero residence time. This singularity arises physically from the quasi-random nature of eddy diffusion at the shortest resolved length and time scales. Although it can be avoided by demanding that fluid elements stay for at least a threshold residence time on the other side of the tropopause before recrossing, the one-way cross-tropopause flux is in practice found to be a sensitive function of threshold time, rapidly increasing with decreasing threshold [*Wernli and Bourqui*, 2002; *Hall and Holzer*, 2003]. In recognition of this, *Orbe et al.* [2012] introduced a robust numerical procedure for obtaining the one-way air mass flux partitioned with respect to stratospheric residence time, τ, and with respect to the regions where air enters the stratosphere and returns to the troposphere.

[5] This partitioned flux, or flux distribution, quantifies the ventilation of the stratosphere much along the lines of the work of *Primeau and Holzer* [2006] for the ventilation of the ocean. The one-way flux distribution thus quantifies the one-way flux without being rendered ill defined by the eddy-diffusive singularity. Note that the net air mass flux of *Holton et al.* [1995] and *Appenzeller et al.* [1996] is not affected by the singularity. However, because of eddy diffusion, large cross-tropopause tracer gradients can lead to significant tracer transport even if the net mass flux is zero, which is why the net mass flux is an incomplete diagnostic [e.g., *Gettelman and Sobel*, 2000; *Nakamura*, 2007].

[6] Here we extend the idealized study of *Orbe et al.* [2012] for statistically stationary flow to comprehensively modeled seasonally varying flow. *Orbe et al.* [2012] used integrations with a dry dynamical core run under perpetual Northern Hemisphere (NH) winter conditions to illustrate the latitude and residence time structure of the climatological zonal mean one-way flux across the thermal tropopause. Here our goal is to determine the one-way air mass fluxes and associated stratospheric residence times for a comprehensively modeled realistic atmosphere, with a focus on seasonal variations.

[7] We calculate one-way stratosphere-to-troposphere flux distributions in the Goddard Earth Observing System Chemistry Climate Model (GEOSCCM). The seasonal forcing, representation of moist thermodynamics, topography, and surface fluxes enable us to quantify STE for a realistic atmosphere in terms of the one-way air mass flux and diagnostics derived therefrom. Special attention is paid to quantifying the seasonality of the flux with respect to the month of year (a) when air enters the stratosphere, (b) when the mass of the stratosphere is partitioned, and (c) when air exits back to the troposphere. Our results provide a benchmark for evaluating the tropopause-to-tropopause transport through the stratosphere in other models.

2. Theory of One-Way Flux Distributions

[8] We quantify one-way STE across the thermal tropopause (see section 3.2). To track air parcels during their transit from where they enter the tropopause at region Ω_i, to the tropopause point of exit, $\mathbf{r}_\Omega$, we use the boundary propagator Green function $\mathcal{G}$ (which has dimensions of inverse time) so that $\mathcal{G}$ may be thought of as a tracer label that is applied to air on Ω_i at t_i and removed at $\mathbf{r}_\Omega$ at time $(t_i, t_i + \mathrm{d}t_i)$. Physically, $\mathcal{G}(\mathbf{r}, t|\Omega_i, t_i)\mathrm{d}t_i$ is the mass fraction of air at position $\mathbf{r}$ and time t that had last Ω_i contact during $(t_i, t_i+\mathrm{d}t_i)$. The quantity $\mathcal{G}$ also has the interpretation of being the age spectrum for air entering the stratosphere at the tropics at time t_i [*Hall and Plumb*, 1994], and to the degree that the flow is statistically stationary, $\mathcal{G}$ is also the distribution of transit times since last contact with the tropopause (i.e., transit time distribution, the distribution of air with times $(t - t_i, t - t_i + \mathrm{d}t_i)$ since last contact with Ω_i).

[9] The boundary propagator $\mathcal{G}$ is computed as the passive tracer response to a pulse in mixing ratio applied on Ω_i during $(t_i, t_i + \mathrm{d}t_i)$ that satisfies the source-free advection-diffusion equation

$$\frac{\partial}{\partial t}(\rho\mathcal{G}) + \nabla \cdot \mathbf{J} = 0, \tag{1}$$

where $\mathbf{J}$ is the advective-diffusive mass flux of $\mathcal{G}$ and ρ is the density of air. For the generic case of advection with velocity $\mathbf{u}$ and Fickian diffusion with diffusivity tensor $\mathbf{K}$, we have $\mathbf{J} = (\rho\mathbf{u} - \rho\mathbf{K}\nabla)\mathcal{G}$. The tropopause boundary conditions for $\mathcal{G}$ [*Holzer and Hall*, 2000] are

$$\mathcal{G}(\mathbf{r}_\Omega, t|\Omega_i, t_i) = \Delta(\mathbf{r}_\Omega, \Omega_i)\delta(t - t_i), \tag{2}$$

where $\delta(t - t_i)$ is the usual Dirac delta function, and the surface mask $\Delta(\mathbf{r}_\Omega, \Omega_i) = 1$ if $\mathbf{r}_\Omega$ lies on Ω_i, and $\Delta(\mathbf{r}_\Omega, \Omega_i) = 0$ otherwise. Note that a boundary condition of zero applies to the entire tropopause for $t > t_i$. This ensures that the $\mathcal{G}$ label is removed on repeat contact with the tropopause. We will also refer to $\mathcal{G}$-labeled air as "Ω_i air".

[10] The one-way S → T air-mass flux through $\mathbf{r}_\Omega$ that has resided in the stratosphere for a time in the interval $(\tau, \tau + \mathrm{d}\tau)$ is given by $\mathcal{J}(\mathbf{r}_\Omega, t_i + \tau|\Omega_i, t_i)\mathrm{d}\tau$, where $\mathcal{J}$ is the component of $\mathbf{J}$ that is normal to the tropopause. Note, however, that we do not calculate these fluxes explicitly;

instead, we use a simple mask-budget approach [*Orbe et al.*, 2012] that is more robust and drastically simplifies our calculations (see experimental design, section 3). Thus, $\mathcal{J}$ is a flux-density distribution that partitions the flux of Ω_i air at t_i and exiting at point $\mathbf{r}_\Omega$ according to residence time τ [*Primeau and Holzer*, 2006]. The boundary conditions (2) ensure that there is no return flux of Ω_i air from the troposphere so that $\mathcal{J}$ is the one-way, or gross, S → T flux with dimensions of mass/area/time^2.

[11] While $\mathcal{J}$ is interesting in itself, *Primeau and Holzer* [2006] show that $\mathcal{J}$ can also be used to obtain the integrable distribution $\mathcal{R}$ defined so that $\mathcal{R}\mathrm{d}\tau\mathrm{d}^2\mathbf{r}_\Omega$ is the mass of the stratosphere in transit at time t that entered at Ω_i and will exit at $\mathbf{r}_\Omega$ after a stratospheric residence time in the interval $(\tau, \tau + \mathrm{d}\tau)$. When Ω_i is the entire tropopause, $\int_{\Omega_i} \mathrm{d}^2\mathbf{r}_\Omega \int_0^\infty \mathrm{d}\tau\ \mathcal{R}$ gives the entire mass of the stratosphere at time t. The residence time distribution, $\mathcal{R}$, (also "transport-mass distribution" [*Holzer and Hall*, 2008]) is given by

$$\mathcal{R}(\tau, \Omega_i, \mathbf{r}_\Omega; t) = \int_{t-\tau}^{t} \mathrm{d}t_i\ \mathcal{J}(\mathbf{r}_\Omega, t_i + \tau | \Omega_i, t_i). \tag{3}$$

Physically, (3) states that the mass in transit at time t whose residence time will lie in the interval $(\tau, \tau + \mathrm{d}\tau)$ consists of air that entered the stratosphere at times t-τ through t and will leave the stratosphere a time τ later at $\mathbf{r}_\Omega$. In the case of steady flow, (3) becomes $\mathcal{R} = \tau\mathcal{J}$, which states that if the steady flux of air whose residence time is in the interval $(\tau + \mathrm{d}\tau)$ acts for a time τ, the mass of the stratosphere in that residence time interval will be flushed out [*Primeau and Holzer*, 2006]. Note that for annually repeating cyclostationary flow, $\mathcal{R}$ depends on t only through $\tilde{t} \equiv t \bmod 1$ year, i.e., only on the time of year at which we partition the mass of the stratosphere.

[12] Because $\mathcal{R}$ partitions the finite mass of the stratosphere, it is integrable even when overlapping entry/exit patches introduce a singularity at $\tau = 0$. Therefore, $\mathcal{R}$ is usefully summarized by its moments. The mass, μ, in transit at time t from Ω_i to $\mathbf{r}_\Omega$ regardless of residence time, τ, is given by

$$\mu(\Omega_i, \mathbf{r}_\Omega; t) = \mathrm{d}^2\mathbf{r}_\Omega \int_0^\infty \mathrm{d}\tau\ \mathcal{R}(\tau, \Omega_i, \mathbf{r}_\Omega; t), \tag{4}$$

where $\mathrm{d}^2\mathbf{r}_\Omega$ is the horizontal area of the grid box at $\mathbf{r}_\Omega$ and the mean $\Omega_i \to \mathbf{r}_\Omega$ residence time is given by

$$\overline{\tau}(\Omega_i, \mathbf{r}_\Omega; t) = \frac{1}{\mu(\Omega_i, \mathbf{r}_\Omega; t)} \mathrm{d}^2\mathbf{r}_\Omega \int_0^\infty \mathrm{d}\tau\ \tau\mathcal{R}(\tau, \Omega_i, \mathbf{r}_\Omega; t). \tag{5}$$

Orbe et al. [2012] point out that $\bar{\tau}$ provides an upper bound on the time available for the mass of the stratosphere in transit from Ω_i to $\mathbf{r}_\Omega$ at time t to be subjected to stratospheric chemistry.

[13] The flux distribution $\mathcal{J}$ is the fundamental transport diagnostic at the core of our analysis. Using a comprehensive general circulation model, we provide the first analysis of quantitatively realistic one-way STE in terms of one-way flux distributions, the mass in transit from $\Omega_i \to \mathbf{r}_\Omega$, and the mean residence time of this mass. We focus, in particular, on the seasonal variations of these transport diagnostics.

3. Experimental Design

3.1. The Model

[14] We use GEOSCCM Version 2, which couples the GEOS5-general circulation model [*Rienecker et al.*, 2008] with a comprehensive stratospheric chemistry package [*Douglass et al.*, 1996]. The model has a horizontal resolution of 2° latitude by 2.5° longitude, with 72 vertical levels extending from the surface to 0.01 hPa. The model is forced with annually repeating 2010 greenhouse gases (GHG) and ozone depleting substances under the A1B and A1 scenarios, respectively [*Intergovernmental Panel on Climate Change*, 2001; *World Meteorological Organization (WMO)*, 2007]. Sea surface temperatures and sea ice concentrations are years 2000–2019 time averages taken from an integration of National Center for Atmospheric Research Community Climate System Model (CCSM) Model 3.0 subject to A1B GHG forcing. Solar forcings are held constant, and there is no representation of the quasi-biennial oscillation (QBO).

[15] Spin-up to a statistically stationary state takes 10 years after which we introduce our diagnostic tracers that are passively advected using a flux-form semi-Lagrangian scheme [*Lin and Rood*, 1996]. There is no explicit tracer diffusion term. Compared to other chemistry climate models, GEOSCCM performs well in terms of its mean stratospheric dynamical and thermal structure, trace gas distributions, and their decadal changes in the recent past [*Eyring et al.*, 2010]. While the model underestimates tropical interannual variability due to the lack of a QBO, this is not expected to impact significantly on mean tropical transport [*Li et al.*, 2012].

3.2. The Diagnostic Tracers

[16] The thermal tropopause is defined using the standard World Meteorological Organization definition [*WMO*, 1957] and computed online for each time step. Because the main pathway from anywhere in the troposphere into the upper stratosphere is through the tropical tropopause, we consider only a single entry region, Ω_i, namely the tropopause from 10°S to 10°N, which is characterized by annual mean upwelling in the tropical lower stratosphere. The boundary conditions (2) are enforced by broadening the delta function to a square pulse of duration $\delta t_i = 30$ days and amplitude $\frac{1}{\delta t_i}$. In practice, $\Delta(\mathbf{r}_\Omega, \Omega_i)$, defined in (2), is extended for numerical convenience throughout the depth of the troposphere [*Orbe et al.*, 2012]. In the case of multiple tropopauses, our procedure captures the lowermost tropopause. This suffices because our resolution is too coarse to resolve all tropopause folds. It is worth noting, however, that our diagnostics can be applied to any surface that separates two domains of the atmosphere, even if that surface is multiply connected with isolated bubbles of air from one domain embedded in the other domain.

[17] Here we explore $\mathcal{J}$ for seasonally varying flow so that $\mathcal{J}$ depends explicitly on (a) when air enters the stratosphere (i.e., entry time t_i) and (b) when air exits the stratosphere (i.e., exit time t_f). Figure 1 shows a schematic of a fluid element traversing the stratosphere. This fluid element is in transit at time t at an interior stratospheric point $\mathbf{r}$, has had a transit time $\xi \equiv t - t_i$ since last tropical tropopause contact, and leaves the stratosphere at t_f after a residence time $\tau \equiv t_f - t_i$.

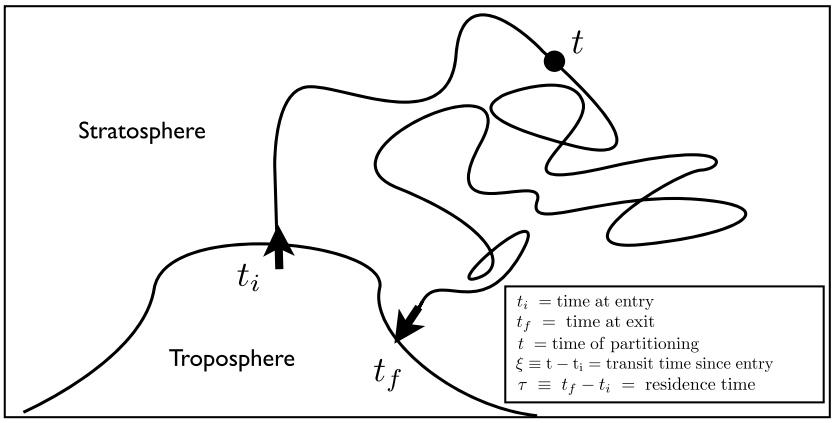

Figure 1. Schematic illustration of tropopause-to-tropopause transport through the stratosphere. Air enters the stratosphere at time t_i, is in transit in the interior of the stratosphere at time t and exits back into the troposphere at time t_f. Air in the interior of the stratosphere at time t has a transit time $\xi \equiv t - t_i$ since last contact with the tropopause; air leaving the stratosphere has resided in the stratosphere a time $\tau \equiv t_f - t_i$ since entering at the tropopause.

[18] In order to probe the seasonal cycle of the one-way flux with respect to entry time t_i, we compute an ensemble consisting of three members. The first ensemble member consists of six pulse tracers, $\mathcal{G}(\mathbf{r}, t|\Omega_i, t_i)$, where t_i = January, March, ..., November in the first year of the model integration following spin-up. The second and third members each consist of six such pulse tracers for the same months in years 2 and 3 of the same integration. Following *Li et al.* [2012], who show that an ensemble of six pulses is sufficient to capture the seasonality of lower stratospheric age spectra in GEOSCCM, we assume that six pulses are also sufficient for capturing the seasonal variability of $\mathcal{J}$. Our choice of the three ensemble members rests on the assumption that the largest variability is primarily seasonal and that interannual

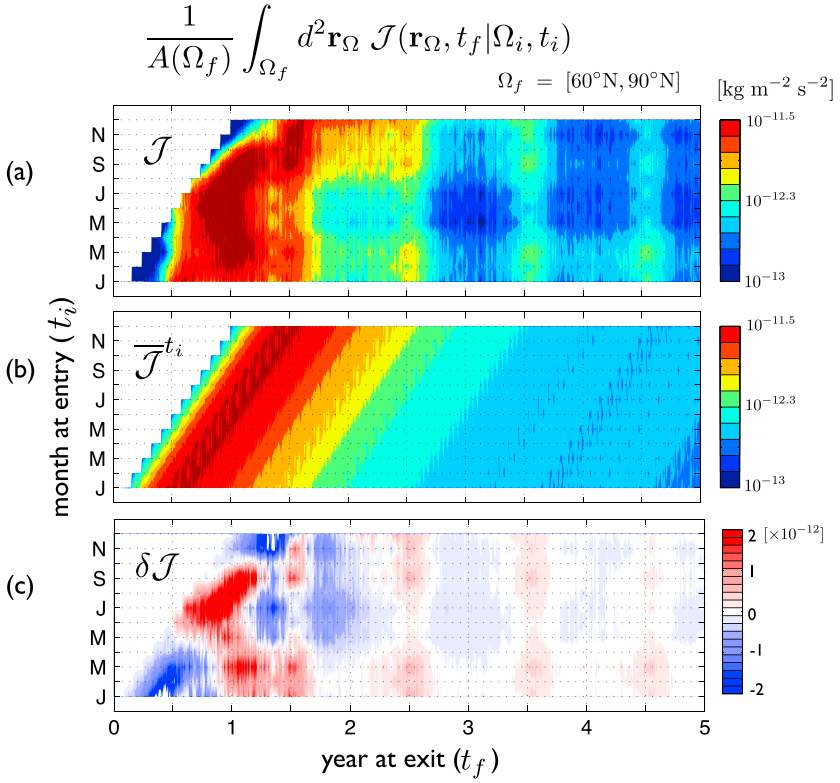

Figure 2. The ensemble mean one-way flux of air that entered the stratosphere through the tropical tropopause Ω_i (a zonal strip between ±10°) at time t_i and leaves poleward of 60°N, averaged over Ω_f = [60°N, 90°N]. (a) The seasonally varying one-way flux is decomposed into (b) a residence time-dependent annual mean component (averaged over entry time t_i at fixed residence time $\tau = t_f - t_i$) and (c) deviations therefrom.

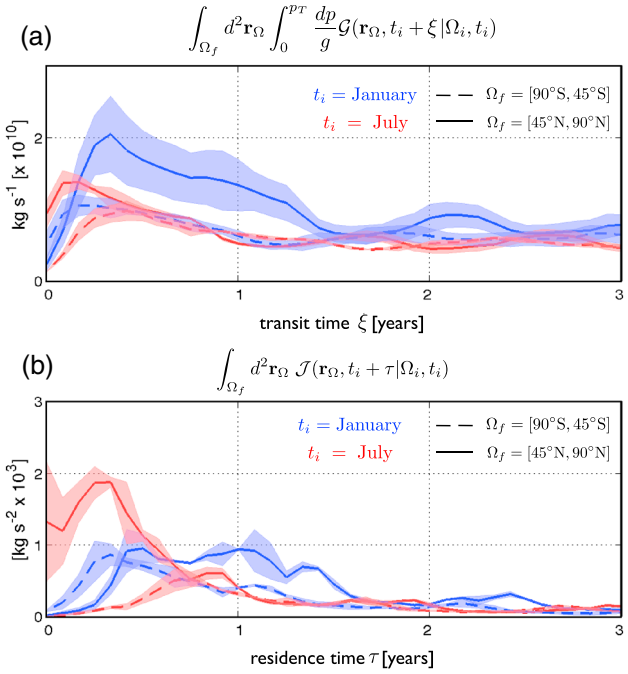

Figure 3. (a) The ensemble-averaged boundary propagator, $\mathcal{G}$, mass integrated over the latitudes poleward of 45° (NH solid, SH dashed) for air that entered the stratosphere in January (blue) and July (red). (b) The one-way flux distribution, $\mathcal{J}$, integrated over the tropopause poleward of 45°N (NH solid, SH dashed). Shading in Figures 3a and 3b denotes one standard deviation from the ensemble mean.

variability is small compared to seasonal variations. This is a reasonable assumption given the lack of a modeled QBO.

[19] For each 30 day pulse, we compute the mass flux per unit residence time, $\mathcal{J}$, as the mass of Ω_i air that crosses back into the troposphere per time step between successive applications of the boundary condition (2) [*Orbe et al.*, 2012]. Equation (1) is integrated for 20 years (following the 10 year spin-up to climatology before our diagnostic tracers are added), consistent with studies by *Schoeberl et al.* [2003] and *Li et al.* [2012], who show that about 20 years are needed to capture the long time scales of stratospheric transport. Integral (3) is evaluated after linearly interpolating $\mathcal{J}$ to monthly t_i values for residence times greater than 1 month and to daily t_i values for smaller residence times so that the small-τ singular behavior is resolved and its contributions to μ and $\bar{\tau}$ accurately captured. The contributions to the integrals in (4) and (5) for $\tau > 30$ years account for roughly 1% of the total residence time integrated flux and are evaluated analytically by extrapolating the exponential tails of $\mathcal{G}$.

3.3. Seasonality of $\mathcal{J}$: Variations With Respect to Entry Time t_i

[20] In order to illustrate the nature of the seasonality of $\mathcal{J}$, we show in Figure 2 the ensemble-averaged and zonally averaged one-way flux distribution, integrated over the NH high latitudes, in the (t_i, t_f) plane. The point of Figure 2 is to demonstrate that the annually averaged flux distribution is defined as an average over the annual cycle with respect to t_i at fixed residence time $\tau = t_f - t_i$. The flux denoted by $\mathcal{J}$ can then be decomposed into this mean (Figure 2b) and deviations therefrom (Figure 2c). Note that the deviations from the annual mean sum to zero along lines of constant τ (the slanted contours of Figure 2b).

[21] In Figure 2b, we introduce notation that designates annual means with respect to the time variable t_x as $\overline{A(t)}^{t_x} \equiv \frac{1}{T}\int_0^T dt\, A(t)$, where t_x is the time variable (either t_i, $\tilde{t}$, or t_f) over which we are averaging at fixed τ, with $T = 1$ year.

4. Results

[22] We present results derived from the ensemble-averaged boundary propagator. Recall that we refer to air entering the stratosphere at the tropics as "Ω_i air". When emphasizing the dependence on entry time, we also refer to this air as "t_i air" (e.g., "January air"). When we assign an uncertainty $\pm\sigma_x$ to quantity X, σ_x represents the standard deviation of X from its three-member ensemble mean.

4.1. Evolution of $\mathcal{G}$

[23] We begin by focusing on January and July air to explore the broad features of the seasonality of STE with respect to entry time t_i. Any significant details that differ for other t_i are noted below.

[24] The evolution of these air masses is in accordance with our understanding of the stratospheric circulation: Air entering the stratosphere at Ω_i undergoes diabatic upwelling in the tropics and isentropic quasi-horizontal transport to high latitudes. We find that 2.9×10^{18} kg more air enters the stratosphere in January than in July (33% more relative to the annual mean) in concert with strong seasonal upwelling at the tropical tropopause during January.

[25] Figure 3 shows the evolution with transit time $\xi \equiv t - t_i$ of the ensemble-averaged boundary propagator, $\mathcal{G}(\mathbf{r}, t|\Omega_i, t_i)$, mass integrated over the stratosphere poleward of 45°N and 45°S. These latitudes are chosen to highlight the transport of Ω_i air to high latitudes; equatorward of these latitudes for small transit times quasi-horizontal transport dominates in the subtropics and rapid eddy-diffusive transport dominates in the tropical entry region.

[26] Figure 3a shows that $\mathcal{G}$-labeled tropical July (JUL) air peaks at a transit time of about 3 weeks in the NH, whereas January (JAN) air peaks at about 4 months. The fact that air that entered in July is more rapidly transported to NH high latitudes is consistent with the boreal summertime weakening of the subtropical mixing barrier that separates the tropics from the extratropics in the lower stratospheric overworld [*Plumb*, 1996; *Neu and Plumb*, 1996; *Li et al.*, 2012]. Several studies have shown that this barrier is most permeable during NH summer [*Konopka et al.*, 2009; *Bonisch et al.*, 2009], enabling air that is confined to the tropics to be spread poleward by eddies. This increased permeability has been associated with the extension of the Asian monsoon summer flow well into the lower stratosphere [*Dunkerton*, 1995; *Dethof et al.*, 1999; *Haynes and Shuckburgh*, 2000; *Randel and Park*, 2006].

[27] After peaking within 1 year of entering, Ω_i air decays exponentially with transit time. This decay quantifies the asymptotic return of stratospheric air to the troposphere where it is unlabeled [e.g., *Prather*, 1996; *Ehhalt et al.*, 2004; *Pan et al.*, 2006; *Holzer*, 2009b]. Similar to the work in *Li et al.* [2012], we find that the decay *e*-folding time of

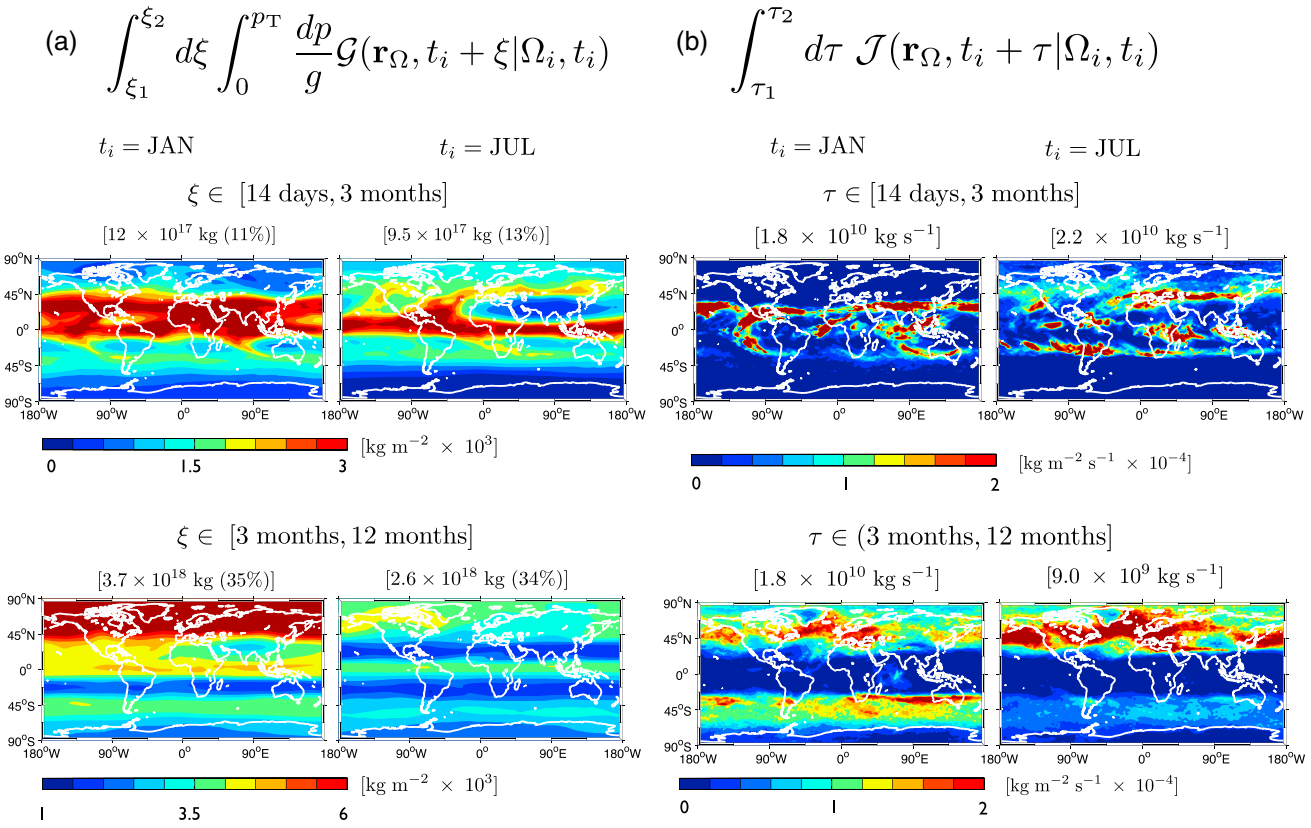

Figure 4. (a) The ensemble-averaged and column-integrated boundary propagator $\mathcal{G}$, mass-averaged over air that has resided in the stratosphere (top) 2 weeks to 3 months and (bottom) 3 to 12 months. (b) The ensemble-averaged one-way S → T air mass flux for air residing in the intervals shown. The globally integrated flux density integrated over residence time band $\tau \in [\tau_1, \tau_2]$ is shown at the top of each map. Air that entered the stratosphere in January and in July are shown in Figures 4a and 4b, respectively. Numbers at the top of each map give the mass of air and the percentage of the incoming air mass that had last Ω_i contact in the transit time interval indicated.

this mode is ∼ 3 years. Figure 3 shows that within 3 years, $\mathcal{G}$ has decayed to 25% of its initial value and variations with entry time t_i have diminished substantially. Because transport into the SH is weaker than into the NH within the first 3 years of entering the stratosphere (Figure 3a), less air returns to the troposphere in the SH and interhemispheric differences rapidly even out during this time.

[28] Figure 4 shows maps of the ensemble-averaged and column-integrated boundary propagator, integrated over various transit time bands, to highlight geographic variations in the transport of Ω_i air (Figure 4a). Within the first 3 months since entry into the stratosphere (Figures 4a, top) Ω_i air is largely confined between the tropics and subtropics, and meridional gradients are largest at the tropospheric jets, particularly in the NH where a greater mass of Ω_i air remains because cross-tropopause transport is strongly suppressed during NH winter [*Chen*, 1995]. Both JAN air and JUL air have prominent minima during NH summer and are centered on the Tibetan Plateau (Figure 4a, top right and bottom left). This feature coincides with the Asian monsoon and is consistent with observations showing localized extrema in upper troposphere/lower stratosphere tracer fields during NH summer, including anomalously high ozone [*Randel and Park*, 2006] and anomalously low water vapor [*Rosenlof et al.*, 1997], methane [*Park et al.*, 2004], and carbon monoxide [*Li et al.*, 2012]. The Asian monsoon is a deep circulation with closed anticyclones extending up to at least 70 hPa in July [*Dunkerton*, 1995]; at this level air remains confined for several weeks compared to only a few days in the middle troposphere and lower stratosphere [*Randel and Park*, 2006]. This confinement suggests that Ω_i air trapped in the stratospheric monsoon flow has relatively ready access to the tropopause and hence remixes with the troposphere more quickly, resulting in the minima visible in Figure 4.

4.2. The One-Way Flux Distribution, $\mathcal{J}$

[29] The fundamental quantity at the core of this study is the ensemble-averaged one-way flux distribution, $\mathcal{J}(\mathbf{r}_\Omega, t_f | \Omega_i, t_i)$, which is simply the flux of $\mathcal{G}$ across the thermal tropopause per unit residence time induced by boundary condition (2). In this section, we first discuss the seasonality of the one-way flux with respect to entry time t_i, and we then consider how the spatial distribution of $\mathcal{J}$ varies with exit time t_f.

[30] We focus first on the behavior of $\mathcal{J}$ for small residence times. The one-way flux of JAN and JUL air with residence times $\tau = t_f - t_i$ of 3 months or less makes up (36±6)% and (55±3)% of the total flux poleward of ±45° (i.e., the return flux regardless of residence time) back into the troposphere. These small-τ fluxes are larger in the NH

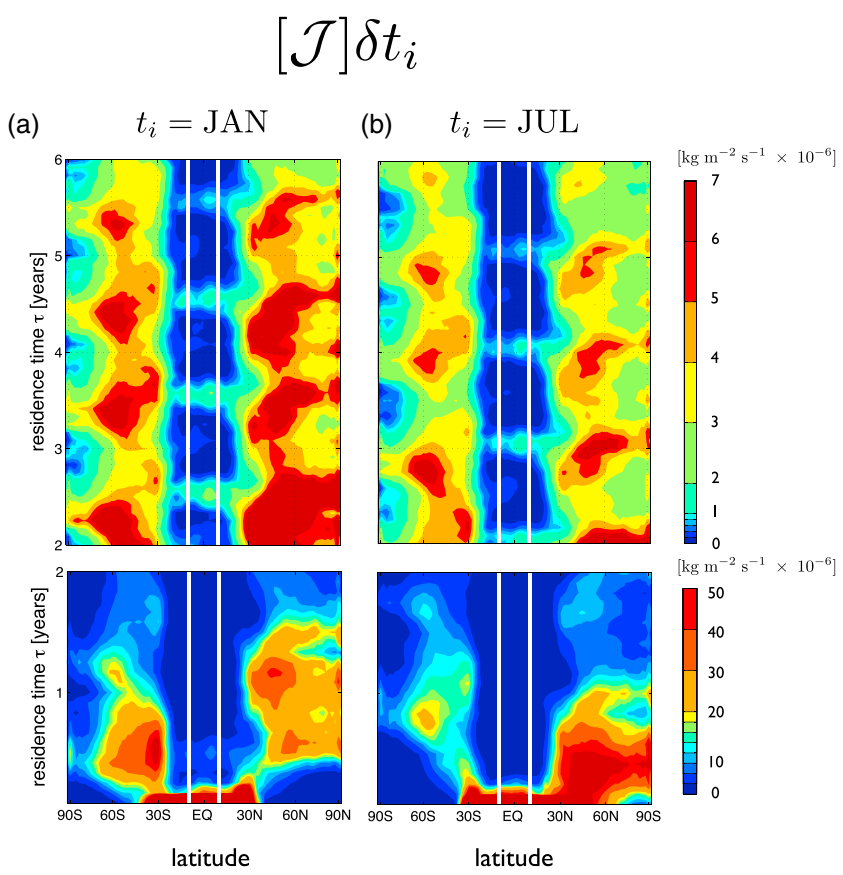

Figure 5. The ensemble-averaged and zonally averaged one-way S → T mass flux , $\mathcal{J}\delta t_i$, that entered the stratosphere during a 30 day time interval δt_i in (a) January and (b) July as a function of exit latitude and stratospheric residence time, τ. Note the two color scales: (bottom) one for air with residence times less than 2 years and (top) the other for residence times greater than 2 years. Two linear color scales are used in order to capture the full dynamic range of $\mathcal{J}$, including the large fluxes at small residence times. The residence time axis is stretched for $\tau < 2$ years so that the large short-τ fluxes, and their rapid decay with τ, are visible. The vertical lines mark the edges of Ω_i.

than in the SH, as shown in Figure 3b, where $\mathcal{J}$ has been separately integrated over each hemisphere poleward of 45°. Consistent with the fact that air is more rapidly transported to NH high latitudes in summer (see section 4.1), we find that the one-way flux across the NH tropopause for air with $\tau < 3$ months is (34±10)% larger for JUL air than for JAN air. The small-τ fluxes back into the troposphere in the SH are larger for JAN air, as expected for SH summertime transport, but the amplitudes of $\mathcal{J}$ for both air masses are overall larger in the NH than in the SH so that, as in section 4.1, we mainly focus on the NH.

[31] The maps of $\mathcal{J}$ in Figure 4b also reveal that the longitudinal structure of one-way STE depends strongly on how long the Ω_i air mass has resided in the stratosphere when $\tau < 1$ year. Air with $\tau < 3$ months is rapidly transported diffusively back across the tropical tropopause or quasi-horizontally across the tropopause of adjacent latitudes (Figure 4b, top). The more familiar storm track pattern, evident in the STE analyses of *Seo and Bowman* [2002], *Sprenger and Wernli* [2003], *Tang and Prather* [2010], and *Tang et al.* [2011], manifests itself for $\tau > 3$ months (Figure 4b, bottom). A few smaller-scale features are also worth pointing out: For JUL-air, enhanced one-way fluxes over Asia and Europe point to the key role that the Asian monsoon plays in ventilating the stratosphere during boreal summer.

[32] Figure 5 shows the zonally averaged flux density $\mathcal{J}$ as a function of exit latitude and residence time. This figure shows that for a few weeks after first entering the stratosphere, $\mathcal{J}$ is overwhelmingly large at the entry region (±10°), as air readily diffuses back through the tropical tropopause, rendering the flux there difficult to estimate robustly unless diagnostics like $\mathcal{J}$ are used that partition the flux explicitly with respect to residence time. (Note that this diffusion is dominantly numerical here, because subgrid diffusion is not explicitly modeled.). A $\tau^{-\frac{3}{2}}$ singularity at $\tau = 0$ is expected for Fickian diffusion in the continuum limit [*Hall and Holzer*, 2003; *Primeau and Holzer*, 2006; *Orbe et al.*, 2012]. In the appendix, we show that the small-τ power law is independent of entry time t_i. With increasing τ, these large fluxes decay rapidly, and within $\tau \sim 200$ days, $\mathcal{J}$ has decayed by 2 orders of magnitude.

[33] For $\tau \geq 2$ years, away from the dominance of the nearly singular behavior, the pattern of $\mathcal{J}$ is strikingly different at midlatitudes than in the tropics. The one-way flux returning across the midlatitude tropopause is made up of air that, at different stages during upwelling in the tropics, crosses the tropical barrier isentropically and spends a broad

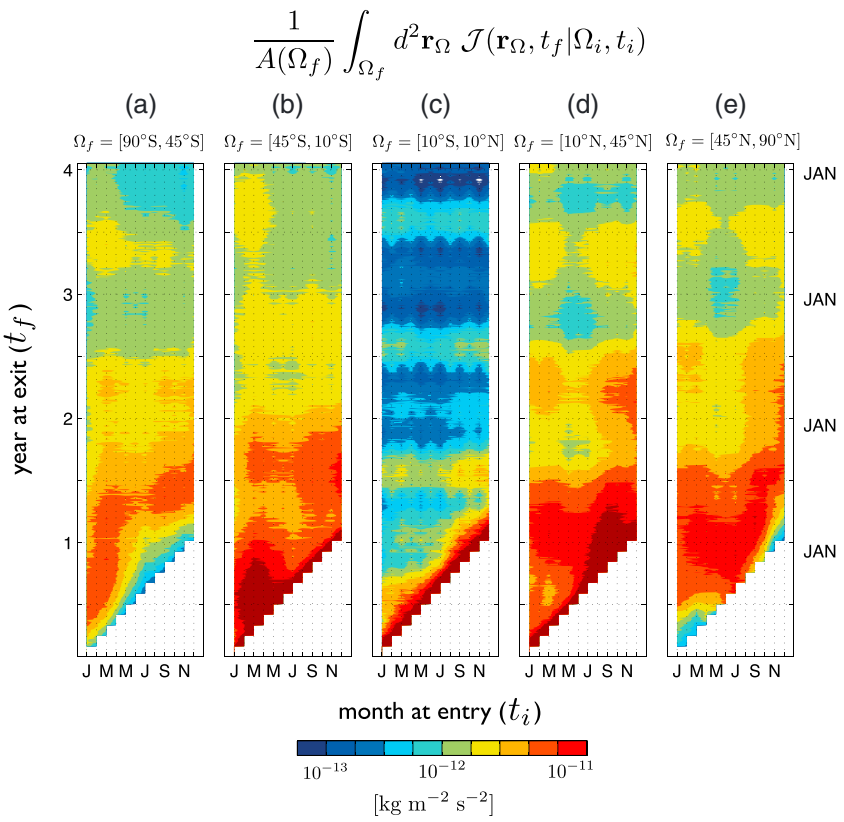

Figure 6. The ensemble-averaged and zonally averaged one-way S → T air mass flux for air entering the stratosphere at times t_i and exiting back to the troposphere at times t_f, averaged over Ω_f spanning (a) the SH high latitudes, (b) the SH midlatitudes, (c) the tropics, (d) the NH midlatitudes, and (e) the NH high latitudes. The vertical axis extends to 4 years in order to capture the strong seasonality of $\mathcal{J}$ with respect to t_i.

range of times recirculating in the extratropical stratosphere before descending back into the troposphere [*Gettelman and Sobel*, 2000; *Seo and Bowman*, 2002; *Holzer*, 2009a; *Orbe et al.*, 2012]. Note that large short-τ fluxes at midlatitudes are associated with rapid isentropic transport to midlatitudes, not with the rapid eddy-diffusive near-singularity, because the midlatitudes do not overlap with the tropical entry region. At larger residence times τ, extratropical fluxes decay exponentially to zero (not shown) as all of the Ω_i air eventually returns to the troposphere. The *e*-folding time for this decay is $\sim$ 3 years.

[34] To further quantify the seasonality of $\mathcal{J}$, it is revealing to examine the evolution of the one-way flux with respect to entry time t_i and exit time t_f. Figure 6 shows $\mathcal{J}(\mathbf{r}_\Omega, t_f | \Omega_i, t_i)$ integrated over five key latitude bands. Large fluxes at midlatitudes are visible for $\tau < 1$ year in both hemispheres for late summer to early autumn entry times (Figures 6b and 6d). The one-way flux at high latitudes also demonstrates strong sensitivity to t_i at small residence times because quasi-isentropic transport to polar regions is suppressed when a strong polar vortex is present. Specifically, polar fluxes are 1 order of magnitude smaller for winter entry times (Figures 6a and 6e) than for summer entry times (within each hemisphere).

[35] While the flux of air with $\tau < 2$ years is seen in Figure 6 to depend strongly on t_i, the one-way flux of older air is only weakly dependent on t_i. July maxima with respect to exit time t_f are seasonally recurring in the tropics and may be explained in terms of the boreal summertime weakening of the tropical-extratropical mixing barrier [*Bonisch et al.*, 2009; *Li et al.*, 2012]. (The seasonally recurring fluxes back into the tropics were noticeably absent in the idealized work of *Orbe et al.* [2012], because the flow was statistically stationary and representative only of perpetual NH winter.). In the subtropics, fluxes peak in late winter to early spring (Figures 6b and 6d) and at high latitudes during late summer (Figures 6a and 6e), independent of entry time. We explain this seasonality in exit time t_f as follows: In late winter/early spring the presence of a strong polar vortex suppresses mixing to high latitudes, which leads to anomalously large fluxes out of the subtropics at the tropopause (i.e., maxima from late winter to early spring). At high latitudes during summer, when the polar vortex is weakest, tropical and subtropical air is free to move into high latitudes without being shunted to low and midlatitudes (i.e., maxima from late summer to early autumn). *Li et al.* [2012] used similar reasoning to explain the seasonality of stratospheric age spectra.

4.3. The Mass of the Stratosphere in Transit From $\Omega_i \rightarrow \mathbf{r}_\Omega$ and its Mean Residence Time

[36] To further distill the rich information contained in the one-way flux distribution, we now focus on the partitioning of the mass of Ω_i air in transit during time of year $\tilde{t}$ according to where the air eventually exits and its residence time in the stratosphere. From this transport-mass distribution we

$$\frac{1}{A(\Omega_f)} \int_{\Omega_f} d^2\mathbf{r}_\Omega \, \mathcal{R}(\tau, \Omega_i, \mathbf{r}_\Omega; t)$$

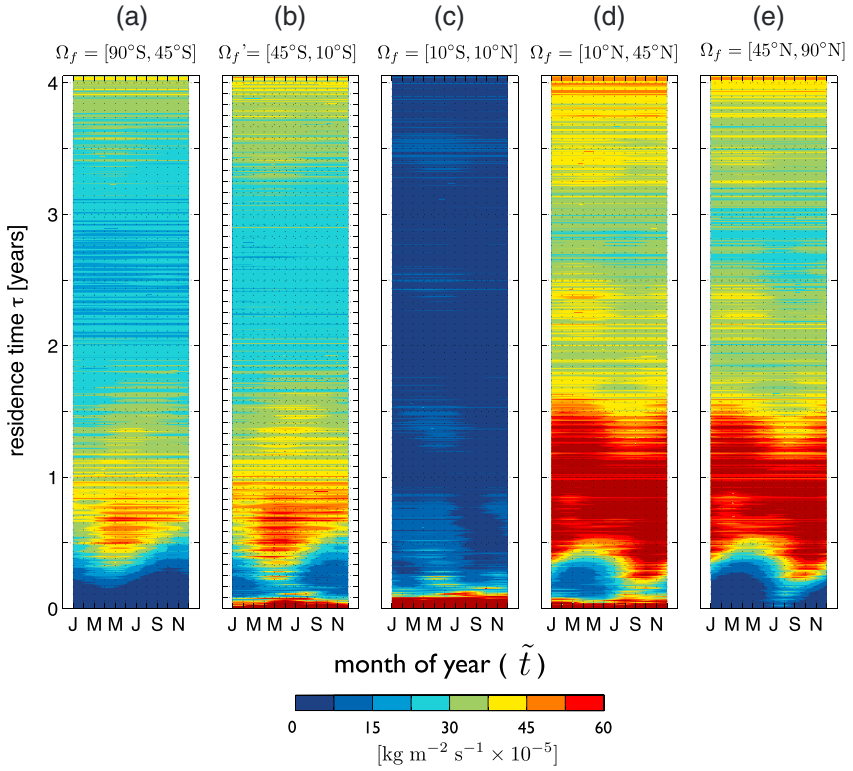

Figure 7. The ensemble-averaged and zonally averaged mass of the stratosphere (per unit residence time) that is in transit from Ω_i to $\mathbf{r}_\Omega$ during month of year $\tilde{t}$ and will leave the stratosphere after a residence time τ, averaged over exit regions Ω_f spanning (a) the SH high latitudes, (b) the SH midlatitudes, (c) the tropics, (d) the NH midlatitudes, and (e) the NH high latitudes. The vertical axis extends to 4 years in order to capture the strong seasonality of $\mathcal{R}$ with respect to $\tilde{t}$.

compute μ, the mass in transit from Ω_i to r_Ω regardless of residence time, and $\bar{\tau}$, the mean residence time (the norm and first temporal moment).

4.3.1. Transport-Mass Distribution, $\mathcal{R}$

[37] Figure 7 shows the $\Omega_i \rightarrow \Omega_f$ transport-mass distribution $\mathcal{R}$ (see equation (3)) as a function of the month of year $\tilde{t}$ during which the Ω_i air mass is being partitioned and as a function of its eventual residence time, τ. We use the same exit regions Ω_f as for Figure 6, for comparison with $\mathcal{J}$. Interestingly, we find that the Ω_i air mass destined to return through these Ω_f regions depends strongly on $\tilde{t}$ only for $\tau \leq 6$ months. For $\tilde{t}$ in late summer to early fall, air with $\tau \leq 6$ months (that is, air that entered the stratosphere anytime from late winter to late summer) is about 6 times more likely to be flushed back into the troposphere than for $\tilde{t}$ in winter to early spring (i.e., air that first entered the stratosphere anytime from summer to late winter). Furthermore, this rapid ventilation is not hemispherically symmetric: Approximately 30% more mass leaves the NH than the SH within the first 6 months. Correspondingly, the amplitude of the seasonal cycle of $\mathcal{R}$ with respect to $\tilde{t}$ is about two thirds smaller in the SH. For $\tau > 6$ months, however, it does not matter during which month we partition the stratosphere: $\int_{\Omega_f} \mathrm{d}^2\mathbf{r}_\Omega \, \mathcal{R}(\tau, \Omega_i, \mathbf{r}_\Omega; \tilde{t})$ is largely independent of $\tilde{t}$ for all exit regions Ω_f.

4.3.2. Total $\Omega_i \rightarrow \mathbf{r}_\Omega$ Mass in Transit, μ, and Mean Residence Time, $\bar{\tau}$

[38] To summarize the information contained in $\mathcal{R}$, we calculate $\mu(\Omega_i, \mathbf{r}_\Omega; \tilde{t})$, the mass of the stratosphere in transit from Ω_i to $\mathbf{r}_\Omega$ during month of year $\tilde{t}$, regardless of residence time defined by equation (4). Figure 8 (left) shows maps of the $\mathbf{r}_\Omega$ dependence of $\mu(\Omega_i, \mathbf{r}_\Omega)$ together with their zonal averages. It turns out that the $\tilde{t}$ dependence of μ is weak. We therefore focus on the annual average with respect to $\tilde{t}$ because $\mathcal{R}$ itself depends strongly on $\tilde{t}$ only for $\tau \leq$ 1 year. One key result evident from Figure 8 is that the largest mass of the stratosphere that enters in the tropics will ultimately leave primarily where (i) it entered (10)% and (ii) through isentropic pathways at midlatitudes, with (51±1)% and (39±2)% leaving between 10°N–90°N and 10°S–90°S, respectively. Except over Ω_i, where the large values of μ are associated with the short-τ diffusive singularity [*Orbe et al.*, 2012], the largest masses return to the troposphere downstream of the storm tracks.

[39] It is useful to contrast μ with previous diagnostics of STE. While the S → T mass fluxes diagnosed from Lagrangian trajectories by *Seo and Bowman* [2002] and *Sprenger and Wernli* [2003] share a broadly similar geographic pattern with μ, their mass fluxes and μ are fundamentally different diagnostics: The fluxes calculated in

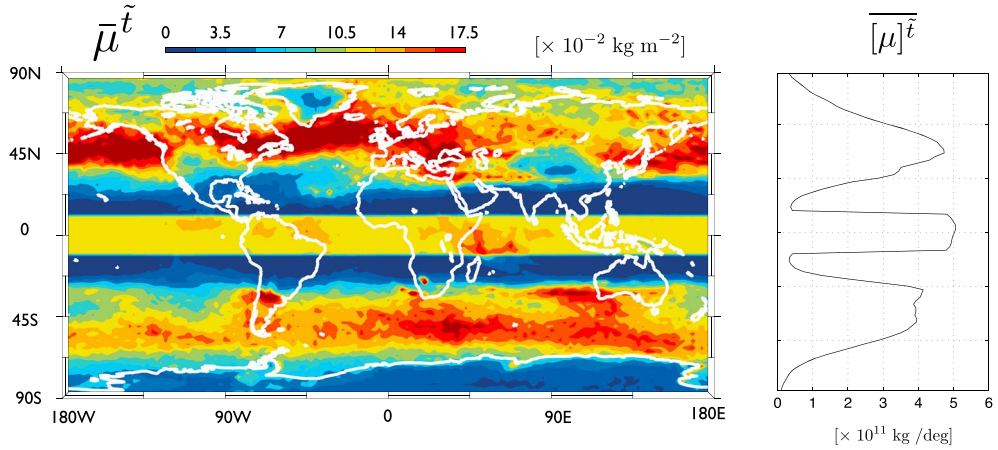

Figure 8. (left) Map of the exit location dependence of the ensemble-averaged mass, μ, of the stratosphere in transit from Ω_i to exit location $\mathbf{r}_\Omega$, independent of when that air is in transit in the stratosphere. We have plotted the mass leaving the stratosphere at $\mathbf{r}_\Omega$ per unit area (m^2) so that, when integrating over the Earth's surface, one recovers the mass leaving the stratosphere that came in at Ω_i. (right) As in the left, except now shown for the zonal mean and plotted in terms of the mass leaving per degree latitude.

those studies are computed for trajectories that start in the interior of the stratosphere, while μ captures the mass of the stratosphere in transit between successive tropopause crossings. It is also worth emphasizing that μ does not suffer from any singularities, and unlike the one-way flux regardless of residence time is well defined for all $\mathbf{r}_\Omega$. Mathematically, $\mathcal{R}(\tau, \Omega_i, \mathbf{r}_\Omega; \tilde{t})$ is integrable with respect to τ for all $\mathbf{r}_\Omega$.

[40] We now consider the mean residence time, $\bar{\tau}$, of $\Omega_i \rightarrow \mathbf{r}_\Omega$ air, defined by equation (5). The mean residence time turns out to have very little variation with longitude because the norm μ is divided out so that the mass whose residence time is computed does not come into play. We therefore consider only zonal averages of $\bar{\tau}$, which are shown in Figure 9. As expected from the singular behavior of $\mathcal{J}$ and $\mathcal{R}$ for small τ and $\mathbf{r}_\Omega \in \Omega_i$, Figure 9a shows that $\bar{\tau} \leq 100$ days over the tropical entry region, which reflects the overwhelming importance of the eddy-diffusive return flux at short residence times. (This behavior was also captured in the idealized experiments of *Orbe et al.* [2012]). Mean residence times increase with latitude to ~ 5 years poleward of $\pm 30^\circ$ and are about 1 year shorter in the NH than in the SH, reflecting the more vigorous flow and residual circulation of the NH. While it is tempting to attribute these shorter mean residence times to differences between the strength of the residual mean circulation of each hemisphere, we emphasize that this can only be a partial

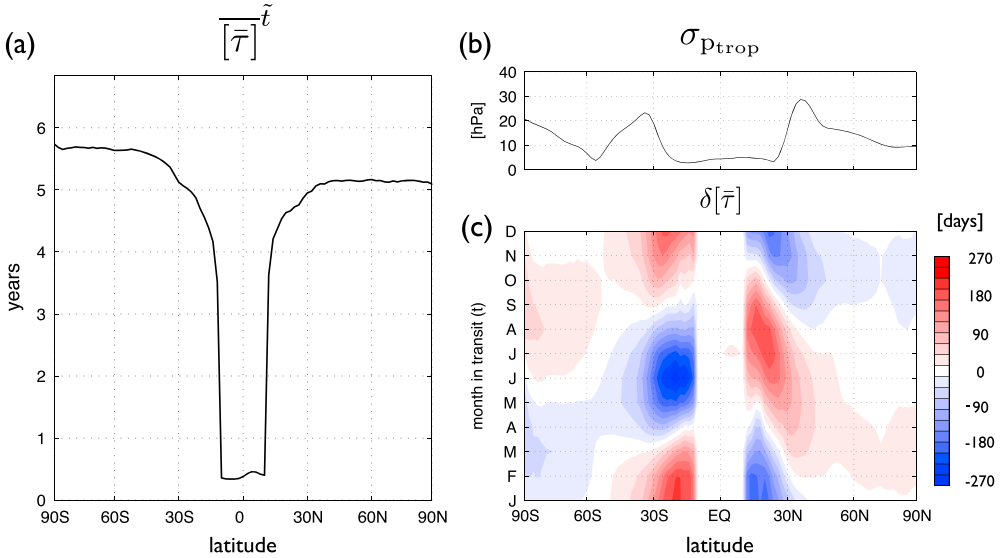

Figure 9. (a) The ensemble-averaged and zonally averaged mean residence time, $\bar{\tau}$, of Ω_i air, annually averaged over the seasonal cycle with respect to $\tilde{t}$, the time of year when the air is being partitioned. (b) Tropopause variability quantified in terms of the standard deviation of tropopause pressure from the annual mean. (c) Ensemble-mean deviations of the seasonally varying mean residence time, $[\bar{\tau}]$, from the annual mean in Figure 9a. Contours are spaced 25 days apart.

explanation. The residual stream function is not sufficient to characterize stratospheric transport, a point that is now widely appreciated in the stratospheric dynamics community [*Plumb*, 2007].

[41] Finally, Figures 9b and 9c show that the residence time of Ω_i air depends modestly on $\tilde{t}$. This seasonality with respect to when the air mass is partitioned is strongest for air leaving the stratosphere in the subtropics: The Ω_i air in transit in summer that is destined to leave in the subtropics will have resided in the stratosphere $\sim$ 200 days longer than such air in transit during the other seasons. One can understand this result by considering integrating $\mathcal{R}$ with respect to τ. The distribution $\mathcal{R}$, shown in Figure 7, depends most strongly on $\tilde{t}$ for $\tau < 1.5$ years and for exit latitudes spanning $\pm(10°, 40°)$ (Figures 7b and 7d). Because mean residence time, $\bar{\tau}$, preferentially weights the contributions made by older air masses, $\bar{\tau}$ is only weakly seasonal outside of the subtropics. Furthermore, the residence time distribution for air that leaves the stratosphere at the subtropics is skewed to larger residence times for $\tilde{t}$ in early spring to early summer compared to other times of the year. For that reason, the Ω_i air in transit in summer that is destined to leave in the subtropics will have resided in the stratosphere $\sim$ 200 days longer than air in transit during other seasons (Figures 9c).

[42] It is important to distinguish mean residence time, $\bar{\tau}$, from stratospheric mean age evaluated at the tropopause, Γ_Ω, which is defined as the first moment of the distribution of transit times from Ω_i to repeat contact with the tropopause [*Holzer et al.*, 2012]. While both time scales are average transit times between entry and exit at the tropopause, *Holzer et al.* [2012] show that Γ_Ω is an average over the population of fluid elements that are exiting the tropopause, whereas $\bar{\tau}$ is an average over all $\Omega \rightarrow \mathbf{r}_\Omega$ fluid elements in the entire stratosphere. Because physically distinct populations of fluid elements are averaged for Γ_Ω and $\bar{\tau}$, the aggregated effects of eddy-diffusive mixing manifest themselves differently.

5. Conclusions

[43] We have quantified the seasonal ventilation of the stratosphere in terms of flux distributions that diagnose the transport of stratospheric air from entry at the tropical tropopause to exit back into the troposphere. This has been accomplished with GEOSCCM, a comprehensive circulation model that provides a realistic representation of the dynamics and transport of the atmosphere [*Eyring et al.*, 2010; *Strahan et al.*, 2011]. The key quantity at the core of our analysis is the one-way flux distribution, $\mathcal{J}$, that partitions the cross-tropopause mass flux of air that entered the stratosphere between $\pm$ 10° according to where this air exits the stratosphere, $\mathbf{r}_\Omega$, and according to its stratospheric residence time, τ. The one-way flux distribution has been shown to capture transport robustly without being rendered ill defined by the short-τ eddy diffusive singularity [*Hall and Holzer*, 2003; *Primeau and Holzer*, 2006; *Orbe et al.*, 2012].

[44] Our previous work on one-way flux distributions exploited simplifications afforded by the statistical stationarity of the modeled flow [*Orbe et al.*, 2012]. However, for realistic atmospheric flows, seasonal variations of the transport add considerable complexity. This seasonality is quantified here with respect to the month of year (a) when air enters the stratosphere, (b) when the mass of the stratosphere is partitioned, and (c) when air exits back into the troposphere. Because of this added complexity, we consider only stratospheric air that entered in the tropics (Ω_i air), not the entire mass of the stratosphere as in *Orbe et al.* [2012]. From the one-way flux distribution, we compute the mass of the stratosphere undergoing $\Omega_i \rightarrow \mathbf{r}_\Omega$ transport and its stratospheric mean residence time. Our main findings are as follows:

[45] 1. The evolution of Ω_i air during its first year in the stratosphere depends strongly on the time of year when entry occurs. For example, nearly *twice* as much JUL Ω_i air is transported to NH high latitudes during its first 3 months since entry compared to JAN Ω_i air. Correspondingly, north of 45°N the flux of Ω_i air back into the troposphere after a residence time $\tau \leq 3$ months is (34$\pm$10)% larger for JUL Ω_i air compared to JAN Ω_i air. This is due to the fact that in the NH JAN Ω_i air tends to remain confined to low latitudes until the subtropical mixing barrier in the lower stratosphere weakens during boreal summer. The longitudinal structure of the flux for $\tau < 1$ year points to the key role that the Asian monsoon plays in rapidly ventilating the stratosphere during boreal summer.

[46] 2. The flow rate of air from Ω_i, through the stratosphere, and back into the SH troposphere is weaker than the flow rate back into the NH troposphere. However, because Ω_i air within the SH is also slower to return to the troposphere, the stratospheric mass of Ω_i air is distributed about evenly between the hemispheres 3 years after entry. After 3 years, 75% of the Ω_i air has returned to the troposphere and its subsequent evolution is dominated by exponential decay with an *e*-folding time of $\sim$ 3 years as it continuously leaves the stratosphere. The corresponding decay of the one-way return flux is modulated by a seasonally recurring component that peaks during summer in the tropics and during spring in the subtropics, moving to high latitudes by late summer. This seasonal phasing between the subtropical and high-latitude peak fluxes is consistent with the seasonal evolution of the polar vortex, which is strongest in midwinter when transport to high latitudes is suppressed.

[47] 3. The Ω_i air mass *regardless* of residence time returns to the troposphere primarily at the midlatitude storm tracks (and also in the tropics due to near singular short-τ diffusive fluxes). Averaged over $\tilde{t}$, the time of year when the air mass in transit is partitioned, we find that (51$\pm$1)% of the Ω_i air mass is destined to return poleward of 10°N, and (39$\pm$2)% is destined to return poleward of 10°S, with the remainder returning in the tropics. The Ω_i air mass leaving in the tropics does so via the near-singular diffusive fluxes, which are purely numerical in our model and hence an aspect of the transport that we cannot reliably quantify. However, the qualitative aspects of these singular fluxes do match theoretical expectations (see Figure 1a), and they are consistent with modeling results in other contexts [*Primeau and Holzer*, 2006; *Holzer*, 2009a, 2009b; *Orbe et al.*, 2012].

[48] 4. In contrast to the Ω_i air mass regardless of residence time, the portion of this mass with residence times less than 6 months depends strongly on the time of year, $\tilde{t}$, during which the air mass is partitioned. Specifically, during September 6 times more Ω_i air with $\tau = 6$ months will leave the NH stratosphere compared to during March. For Ω_i

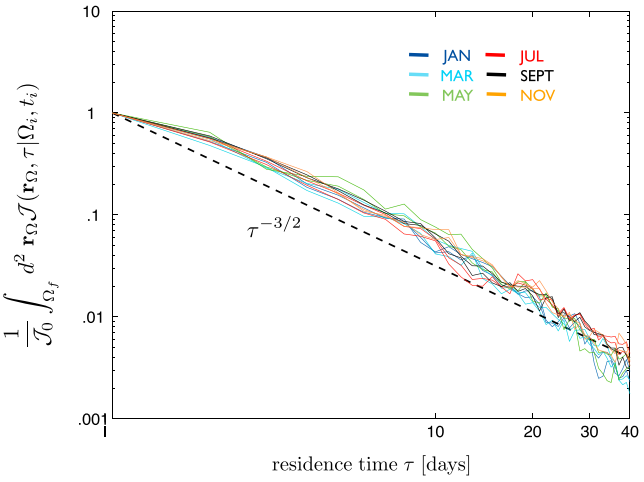

Figure A1. Power law scaling of the area-integrated return flux $\mathcal{J}$ back through the tropical entry region between 10°S and 10°N for small stratospheric residence time, τ. Six lines are shown for air entering the stratosphere in January, March, ..., November. The curves have been normalized by $\mathcal{J}_0$, the value of $\mathcal{J}$ for τ = 1 day.

air with residence times longer than 6 months, however, this seasonality with respect to $\tilde{t}$ is nearly negligible: During any month of year the stratosphere contains similar Ω_i air mass fractions with $\tau > 6$ months that are destined for a given exit region. Consequently, the $\Omega_i \rightarrow \mathbf{r}_\Omega$ air mass regardless of residence time, μ, has only weak seasonality with respect to $\tilde{t}$.

[49] 5. The annually and zonally averaged mean residence time, $\bar{\tau}$, of air undergoing $\Omega_i \rightarrow \mathbf{r}_\Omega$ transport is roughly zero in the tropics and increases sharply with latitude to a nearly constant value of 5.7±0.2 years poleward of 45°S and 5.1±0.1 years poleward of 45°N. Because $\bar{\tau}$ is independent of the mass for which it represents an average, variations of $\bar{\tau}$ with longitude are negligible. The residence time of Ω_i air has modest seasonality with respect to the month of year during which the air mass is partitioned. This seasonality is strongest for air leaving the stratosphere in the subtropics with an amplitude of $\sim$ 20% of the annual mean.

[50] The main point of this paper has been to apply a new tracer independent diagnostic of stratospheric transport to the comprehensively modeled flow of GEOSCCM. The flux distributions represent the one-way flux of air, and not of any particular trace species. However, to model specific trace gases, the flux distributions and their underlying boundary propagators can be convolved with tracer boundary conditions at the tropopause, weighted with decay functions of the time spent in the stratosphere. In this way our diagnostics can be used to disentangle the role of transport from that of chemistry.

[51] Finally, recent studies have shown that future changes in STE will have important implications for the distribution of ozone [*Hegglin and Shepherd*, 2009; *Zeng et al.*, 2010], for the oxidizing capacity of the troposphere [e.g., *Kentarchos and Roelofs*, 2003], and for tropospheric air quality [e.g., *Stohl et al.*, 2000; *Cooper et al.*, 2005]. It is therefore important to quantify how STE will change with the climate, and this will be explored in future work.

Appendix A

[52] Here we show the short-τ dependence of $\mathcal{J}(\Omega_f,\tau|\Omega_i,t_i)$ on τ for $\Omega_f = \Omega_i$ for six different entry times t_i into the stratosphere. Plotted is the area average of $\mathcal{J}(\Omega_f,\tau|\Omega_i,t_i)$ over $\Omega_f = \Omega_i$ = [10°S, 10°N] as a function of τ for 1 day $\leq \tau \leq$ 40 days. For clarity, all curves have been normalized by $\mathcal{J}_0$, the flux at τ = 1 day. The dashed line indicates a $\tau^{-\frac{3}{2}}$ power law to guide the eye and shows that, remarkably, $\mathcal{J}$ diverges approximately like $\tau^{-3/2}$ as $\tau \rightarrow 0$, as expected for Fickian diffusion [*Hall and Holzer*, 2003; *Orbe et al.*, 2012]. This implies that the combination of resolved eddy diffusion and numerical diffusion in GEOSCCM results in simple downgradient diffusion. This "Fickian divergence" is seen to be insensitive to the time of year (t_i) during which the air entered through Ω_i.

[53] **Acknowledgment.** This work was supported by an NSF grant ATM-0854711 (M.H. and L.P.).

References

Abalos, M., W. J. Randel, and E. Serrano (2012), Variability in upwelling across the tropical tropopause and correlations with tracers in the lower stratosphere, *Atmos. Chem. Phys. Discuss.*, *12*, 18,817–18,851, doi:10.5194/acpd-12-18817-2012.

Appenzeller, C., J. R. Holton, and K. H. Rosenlof (1996), Seasonal variation of mass transport across the tropopause, *J. Geophys. Res.*, *101*, 15,071–15,078.

Bonisch, H., A. Engel, J. Curtius, T. Birner, and P. Hoor (2009), Quantifying transport into the lowermost stratosphere using simultaneous in situ measurements of SF6 and CO2, *Atmos. Chem. Phys.*, *9*, 5905–5919, doi:10.5194/acp-9-5905-2009.

Chen, P. (1995), Isentropic cross-tropopause mass exchange in the extra tropics, *J. Geophys. Res.*, *100*, 16,661–16,673.

Cooper, O. R., et al. (2005), Direct transport of midlatitude stratospheric ozone into the lower troposphere and marine boundary layer of the tropical Pacific ocean, *J. Geophys. Res.*, *110*, D23310, doi:10.1029/2005JD005783.

Danielsen, E. F., and V. Mohnen (1977), Project dust storm report: Ozone transport, in situ measurements and meteorological analysis of tropopause folding, *J. Geophys. Res.*, *82*, 5867–5877.

Dethof, A., A. O'Neill, J. M. Slingo, and H. G. J. Stair (1999), A mechanism for moistening the lower stratosphere involving the Asian summer monsoon, *Q. J. R. Meteorol. Soc.*, *125*, 1079–1106.

Dibb, J. E., R. W. Talbot, and G. L. Gregory (1992), 7Be and 210Pb in the western hemisphere Arctic atmosphere: Observations from three recent aircraft-based sampling programs, *J. Geophys. Res.*, *97*, 16,709–16,715.

Douglass, A. R., C. J. Weaver, R. B. Rood, and L. Coy (1996), A three dimensional simulation of the ozone annual cycle using winds from a data assimilation system, *J. Geophys. Res.*, *101*, 1463–1474, doi:10.1029/95JD02601.

Dunkerton, T. J. (1995), Evidence of meridional motion in the summer lower stratosphere adjacent to monsoon regions, *J. Geophys Res.*, *100*, 16,675–16,688.

Ehhalt, D. H., F. Rohrer, S. Schauffler, and M. Prather (2004), On the decay of stratospheric pollutants: Diagnosing the longest-lived eigenmode, *J. Geophys. Res.*, *109*, D08102, doi:10.1029/2003JD004029.

Eyring, V., T. G. Shepherd, and D. W. Waugh, (2010), SPARC Report on the Evaluation of Chemistry-Climate Models, *SPARC Report No. 5, (WMO/TD No. 1526*, World Climate Research Programme (WCRP), 132.

Fry, L. M., F. A. Jew, and P. K. Kuroda (1960), On the stratospheric fallout of strontium 90: The spring peak of 1959, *J. Geophys. Res.*, *65*, 2061–2066.

Gettelman, A., and A. H. Sobel (2000), Direct diagnoses of stratosphere-troposphere exchange, *J. Atmos. Sci.*, *57*, 3–16, doi:10.1175/1520-0469.

Hall, T. M., and M. Holzer (2003), Advective-diffusive mass flux and implications for stratosphere-troposphere exchange, *Geophys. Res. Lett.*, *30*(5), 1222, doi:10.1029/2002GL016419.

Hall, T. M., and R. A. Plumb (1994), Age as a diagnostic of stratospheric transport, *J. Geophys. Res.*, *99*, 1059–1070, doi:10.1029/93JD03192.

Haynes, P., and E. Shuckburgh (2000), Effective diffusivity as a diagnostic of atmospheric transport. Part I: Stratosphere, *J. Geophys. Res*, *105*, 22,777–22,794.

Hegglin, M. I., and T. G. Shepherd (2009), Large climate-induced changes in ultraviolet index and stratosphere-to-troposphere ozone flux, *Nat. Geosci.*, *2*, 687–691, doi:10.1038/ngeo604.

Hegglin, M. I., D. Brunner, T. Peter, P. Hoor, H. Fischer, J. Staehelin, M. Krebsbach, C. Schiller, U. Parchatka, and U. Weers (2006), Measurements of NO, NOy, N2O, and O3 during SPURT: Implications for transport and chemistry in the lowermost stratosphere, *Atmos. Chem. Phys.*, *6*, 1331–1350.

Holton, J. R., P. H. Haynes, A. R. Douglass, R. B. Rood, and L. Pfister (1995), Stratosphere-troposphere exchange, *Rev. Geophys.*, *33*(4), 403–439.

Holzer, M. (2009a), The path density of interhemispheric surface-to-surface transport. Part I: Development of the diagnostic and illustration with an analytic model, *J. Atmos. Sci.*, *66*, 2159–2171, doi:10.1175/2009JAS2894.1.

Holzer, M. (2009b), The path density of interhemispheric surface-to-surface transport. Part II: Transport through the troposphere and stratosphere diagnosed from NCEP data, *J. Atmos. Sci.*, *66*, 2172–2189, doi:10.1175/2009JAS2895.1.

Holzer, M., and T. M. Hall (2000), Transit-time and tracer-age distributions in geophysical flows, *J. Atmos. Sci.*, *57*, 3539–3558.

Holzer, M., and T. M. Hall (2008), Tropospheric transport climate partitioned by surface origin and transit time, *J. Geophys. Res.*, *113*, D08104, doi:10.1029/2007JD009115.

Holzer, M., C. Orbe, and F. Primeau (2012), Stratospheric mean residence time and mean age on the tropopause: Connections and implications for observational constraints, *J. Geophys. Research*, *117*, D12314, doi:10.1029/2012JD017547.

Hsu, J., M. J. Prather, and O. Wild (2005), Diagnosing the stratosphere-to-troposphere flux of ozone in a chemistry transport model, *J. Geophys. Res.*, *110*, D19305, doi:10.1029/2005JD006045.

Intergovernmental Panel on Climate Change (2001), *Climate Change 2001: The Scientific Basis, Contribution of Working Group I to the Third Assessment Report of the Intergovernmental Panel on Climate Change*, edited by J. T. Houghton et al., Cambridge Univ. Press, New York.

Jing, P., D. M. Cunnold, E. S. Yang, and H. J. Wang (2005), Influence of isentropic transport on seasonal ozone variations in the lower stratosphere and subtropical upper troposphere, *J. Geophys. Res.*, *110*, D10110, doi:10.1029/2004JD005416.

Kentarchos, A. S., and G. J. Roelofs (2003), A model study of stratospheric ozone in the troposphere and its contribution to tropospheric OH formation, *J. Geophys. Res.*, *108*(D12), 8517, doi:10.1029/2002JD002598.

Konopka, P., J. Groob, F. Ploger, and R. Muller (2009), Annual cycle of horizontal in-mixing into the lower tropical stratosphere, *J. Geophys. Res.*, *114*, D19111, doi:10.1029/2009JD011955.

Li, F., D. W. Waugh, A. R. Douglass, P. A. Newman, S. Pawson, R. S. Stolarski, S. E. Strahan, and J. E. Nielsen (2012), Seasonal variations of stratospheric age spectra in the Goddard Earth Observing System Chemistry Climate Model (GEOSCCM), *J. Geophys. Res.*, *117*, D05134, doi:10.1029/2011JD016877.

Liang, Q., R. S. Stolarski, A. R. Douglass, P. A. Newman, and J. E. Nielsen (2008), Evaluation of emissions and transport of CFCs using surface observations and their seasonal cycles and the GEOS CCM simulation with emissions-based forcing, *J. Geophys. Res.*, *113*, D14302, doi:10.1029/2007JD009617.

Liang, Q., A. R. Douglass, B. N. Duncan, R. S. Stolarski, and J. C. Witte (2009), The governing processes and timescales of stratosphere-to-troposphere transport and its contribution to ozone in the Arctic troposphere, *Atmos. Chem. Phys.*, *9*, 3011–3025.

Lin, S., and R. Rood (1996), Multidimensional flux-form semi-Lagrangian transport schemes, *Mon. Weather Rev.*, *124*, 2046–2070, doi:10.1175/1520-0493.

McCormick, M. P., L. W. Thomason, and C. R. Trepte (1995), Atmospheric effects of the Mt Pinatubo eruption, *Nature*, *373*, 399–404, doi:10.1038/373399a0.

Monks, P. S. (2000), A review of the observations and origins of the spring ozone maximum, *Atmos. Env.*, *34*, 3545–3561.

Morgenstern, O., and G. D. Carver (2001), Comparison of cross-tropopause transport and ozone in the upper troposphere and lower stratosphere region, *J. Geophys. Res*, *106*(D10), 10,205–10,221, doi:10.1029/2000JD900802.

Mote, P. W., K. H. Rosenlof, M. E. McIntyre, E. S. Carr, J. C. Gille, J. R. Holton, J. S. Kinnersley, H. C. Pumphrey, J. M. Russell III, and J. W. Waters (1996), An atmospheric tape recorder: The imprint of tropical tropopause temperatures on stratospheric water vapor, *J. Geophys. Res.*, *101*, 3898–4006.

Nakamura, N. (2007), Extratropical stratosphere-troposphere mass exchange associated with isentropic mixing: A 1992-2005 climatology derived from advection-diffusion calculations, *J. Geophys. Res.*, *112*, D24303, doi:10.1029/2006JD008382.

Neu, J. L., and R. A. Plumb (1996), Age of air in a "leaky pipe" model of stratospheric transport, *J. Geophys. Res.*, *104*, 19,243–19,255.

Nevison, C. D., D. E. Kinnison, and R. F. Weiss (2004), Stratospheric influences on the tropospheric seasonal cycles of nitrous oxide and chlorofluorocarbons, *Geophys. Res. Lett.*, *31*, L20103, doi:10.1029/2004GL020398.

Olsen, M. A., A. R. Douglass, and M. R. Schoeberl (2003), A comparison of Northern and Southern Hemisphere cross-tropopause ozone flux, *Geophys. Res. Lett.*, *30*(7), 1412, doi:10.1029/2002GL016538.

Orbe, C., M. Holzer, and L. M. Polvani (2012), Flux distributions as robust diagnostics of stratosphere-troposphere exchange, *J. Geophys. Res.*, *117*, D01302, doi:10.1029/2011JD016455.

Pan, L. L., P. Konopka, and E. V. Browell (2006), Observations and model simulations of mixing near the extratropical tropopause, *J. Geophys. Res.*, *111*, D05106, doi:10.1029/2005JD006480.

Park, M., W. J. Randel, D. E. Kinnison, R. R. Garcia, and W. Choi (2004), Seasonal variation of methane, water vapor, and nitrogen oxides near the tropopause: Satellite observations and model simulations, *J. Geophys. Res.*, *109*, D03302, doi:10.1029/2003JD003706.

Plumb, R. A. (1996), A "tropical pipe" model of stratospheric transport, *J. Geophys. Res.*, *101*, 3957–3972.

Plumb, R. A (2007), Stratospheric transport, *J. Meteor. Soc. Japan*, *80*, 793–809.

Prather, M. J. (1996), Natural modes and time scales in atmospheric chemistry: Theory, GWPs for CH4and CO, and runaway growth, *Geophys. Res. Lett.*, *23*, 2597–2600.

Primeau, F. W., and M. Holzer (2006), The oceans memory of the atmosphere: Residence-time and ventilation-rate distributions of water masses, *J. Phys. Oceanogr.*, *36*, 1440–1456.

Randel, W. J., M. Park, F. Wu, and N. Livesey (2007), A large annual cycle in ozone above the tropical tropopause linked to the Brewer-Dobson circulation, *J. Atmos. Sci.*, *64*, 4479–4488.

Randel, W. J., and M. Park (2006), Deep convective influence on the Asian summer monsoon anticyclone and associated tracer variability observed with Atmospheric Infrared Sounder (AIRS), *J. Geophys. Res.*, *111*, D12314, doi:10.1029/2005JD006490.

Rienecker, M. M., et al., (2008), The GEOS-5 data assimilation system—Documentation of versions 5.0.1, 5.1.0, and 5.2.0, *NASA Tech. Memo., NASA TM-2008-104606, vol. 27,* pp. 118, Goddard Space Flight Center Greenbelt, Maryland 20771.

Rosenlof, K. H., A. F. Tuck, K. K. Kelly, J. M. Russell III, and M. P. McCormick (1997), Hemispheric asymmetries in water vapor and inferences about transport in the lower stratosphere, *J. Geophys. Res.*, *102*, 13,213–13,234.

Schoeberl, M. R., A. R. Douglass, Z. Zhu, and S. Pawson (2003), A comparison of the lower stratospheric age spectra derived from a general circulation model and two data assimilation systems, *J. Geophys. Res.*, *108*(D3), 4113, doi:10.1029/2002JD002652.

Schoeberl, M. R., et al. (2008a), QBO and annual cycle variations in tropical lower stratosphere trace gases from HALOE and Aura MLS observations, *J. Geophys. Res.*, *113*, D05301, doi:10.1029/2007JD008678.

Schoeberl, M. R., A. R. Douglass, R. S. Stolarski, S. Pawson, S. E. Strahan, and W. Read (2008b), Comparison of lower stratospheric tropical mean vertical velocities, *J. Geophys. Res.*, *113*, D24109, doi:10.1029/2008JD010221.

Seo, K., and K. P. Bowman (2002), Lagrangian estimate of global stratosphere-troposphere mass exchange, *J. Geophys. Res.*, *107*(D21), 4555, doi:10.1029/2002JD002441.

Sprenger, M., and H. Wernli (2003), A northern hemispheric climatology of cross-tropopause exchange for the ERA15 time period (1979-1993), *J. Geophys. Res.*, *108*(D12), 8521, doi:10.1029/2002JD002636.

Stohl, A., N. Spichtinger-Rakowsky, P. Bonasoni, H. Feldmann, M. Memmesheimer, H. E. Scheel, T. Trickl, S. Hubener, W. Ringer, and M. Mandl (2000), The influence of stratospheric intrusions on alpine ozone concentrations, *Atmos. Environ.*, *34*, 1323–1354.

Stohl, A., H. Wernli, P. James, M. Bourqui, C. Forster, M. A. Liniger, P. Seibert, and M. Sprenger (2003), A new perspective of stratosphere-troposphere exchange, *Bull. Am. Meteorol. Soc.*, *84*(11), 1565–1573.

Strahan, S. E., et al. (2011), Using transport diagnostics to understand chemistry climate model ozone simulations, *J. Geophys. Res.*, *116*, D17302, doi:10.1029/2010JD015360.

Tang, Q., and M. J. Prather (2010), Correlating tropospheric column ozone with tropopause folds: The Aura-OMI satellite data, *Atmos. Chem. Phys.*, *10*(19), 9681–9688, doi:10.5194/acp-10-9681-2010.

Tang, Q., M. J. Prather, and J. Hsu (2011), Stratosphere-troposphere exchange ozone flux related to deep convection, *Geophys. Res. Lett.*, *38*, L03806, doi:10.1029/2010GL046039.

Wernli, H., and M. Bourqui (2002), A Lagrangian "1-year climatology" of (deep) cross-tropopause exchange in the extratropical Northern Hemisphere, *J. Geophys. Res.*, *107*(D2), ACL 13-1–ACL 13-16, doi:10.1029/2001JD000812.

World Meteorological Organization (WMO) (1957), *Meteorology a Three-Dimensional Science: Second Session of the Commission for Aerology, WMO Bulletin IV(4)*, pp.134–138, WMO, Geneva.

World Meteorological Organization (WMO) (2007), *Scientific Assessment of Ozone Depletion:2006*, Global Ozone Res. Monit. Project Rep.50, Geneva, Switzerland.

Zeng, G., O. Morgenstern, P. Braesicke, and J. A. Pyle (2010), Impact of stratospheric ozone recovery on tropospheric ozone and its budget, *Geophys. Res. Lett.*, *37*, L09805, doi:10.1029/2010GL042812.